

Analytical Methods

Accepted Manuscript



This is an *Accepted Manuscript*, which has been through the Royal Society of Chemistry peer review process and has been accepted for publication.

Accepted Manuscripts are published online shortly after acceptance, before technical editing, formatting and proof reading. Using this free service, authors can make their results available to the community, in citable form, before we publish the edited article. We will replace this *Accepted Manuscript* with the edited and formatted *Advance Article* as soon as it is available.

You can find more information about *Accepted Manuscripts* in the [Information for Authors](#).

Please note that technical editing may introduce minor changes to the text and/or graphics, which may alter content. The journal's standard [Terms & Conditions](#) and the [Ethical guidelines](#) still apply. In no event shall the Royal Society of Chemistry be held responsible for any errors or omissions in this *Accepted Manuscript* or any consequences arising from the use of any information it contains.

ARTICLE

Parallelized label-free detection of protein interactions using a hyper-spectral imaging system

Cite this: DOI: 10.1039/x0xx00000x

H. Yoshikawa^a, M. Murahashi^a, M. Saito^a, S. Jiang^a, M. Iga^b, and E. Tamiya^a

Received 00th January 2012,
Accepted 00th January 2012

DOI: 10.1039/x0xx00000x

www.rsc.org/

We describe a Parallelized label-free detection of protein interactions using a hyper-spectral imaging system. Multi-array protein chips were fabricated by immobilizing antibodies on Au-capped nanopillar polymer films, which showed an optical absorption band due to a localised surface plasmon resonance (LSPR) in the absorption spectrum. A parallel detection of multiple antigen-antibody interactions was demonstrated by processing hyper-spectral images of the multi-array chip before and after the application of antigens. Human immunoglobulin A (IgA) and human C-reactive protein (CRP) were specifically detected, and the signal corresponding to these protein concentrations was obtained, indicating that this technique is promising for use in enhancing the performance of multiple protein assays.

Introduction

Multiple screening of different proteins with one chip has become important for diagnostics and bioanalytical applications in recent years. Various platforms have been proposed and studied¹⁻⁶. A multifunctional array platform with high sensitivity, efficiency, and specificity meets the requirement of most medical clinics or laboratory analysts. In particular, a label-free optical detection system using a localised surface plasmon resonance (LSPR) is fascinating for multiple screening applications because of the simplicity of the detection system. LSPR is based on the resonant oscillation of conductive electrons in noble metal nanoparticles excited by light electromagnetic field. Therefore, the fabrication of nanostructures is a key issue for the development of LSPR biosensors. Nanoimprint technology has been recognised as one of the promising methods for the mass production of nano-substrate devices. This was proposed by Chou and co-workers in 1995^{7, 8}. Nanoimprint technology allows the design of a nanometer pattern with sub-10 nm resolution in feature size and with critical dimension control at low-cost, high throughput, large area, and good reproducibility^{9, 10}. Nanoimprint technology has been applied to a fabrication process for a variety of devices such as single electron transistors¹¹, magnetic memory disks¹², and optical devices¹³⁻¹⁵. In many cases, optical biosensing might be the first benefit of this conventional technique. By controlling the polymer nature, we can expect the desired optical functionality in a polymer film that has a nanostructure with a pitch close to the optical wavelength¹⁶. We previously demonstrated the possibility of biosensing¹⁵. We proposed self-ordered anodic alumina oxide (AAO) as a nanostructure mould for nanoimprint to fabricate biosensing substrates at low cost and with large area, size tuning capability,

and ease of the anodizing process that may enhance the production and marketability of nanoimprint technology. Thus, the application of nanoimprint technology to multiple screening is fascinating.

Multiple LSPR biosensing can be performed by using a commercial optical fibre probe for reflection measurements with a simple optical setup³. However, the reflection spectrum from each sensing spot must be measured one by one using a fibre probe. Such a sequential measurement is time-consuming and the time lag between the detection of the first and last spots in a multi-array chip would result in considerable errors in the assay result. Thus multiple screening requires high-throughput. Therefore, Parallelized detection of multiple sensing spots is ideal for multiple screening. Recently, a couple of reports on Parallelized label-free detection with multiple array chips have been published, thus reflecting the urgent need for the technology¹⁷⁻²⁵. In this paper, we performed the multiple detection of antigen-antibody interactions with Au-capped nanopillar chips fabricated by the nanoimprint technique and a hyper-spectral imaging system.

Experimental

Fabrication of the Au-capped nanopillar polymer film

The Au-capped nanopillar polymer film was used as a substrate for the multi-array chip. The fabrication process has already been described in detail¹⁵. Briefly, the porous alumina used as a mould was prepared by an anodic aluminium oxidation. The nanopillar pattern was transferred from the porous structure of the alumina mould to cyclo-olefin polymer (COP) film (Zeon Corp.) by thermal nanoimprint lithography (NIL). Nanoimprint was carried out with a pressure of 2.0 MPa at 160°C (the glass-

transition temperature of COP) for 10 min. A plate seal with holes (3 mm in diameter) was placed on the nanopillar polymer film. The Au-capped nanopillar structure was formed by the deposition of a 68 nm Au film on the imprinted COP surface by sputtering (ACS4000, ULVAC Inc.). The Au-capped nanopillar film was cut to an optional size (about 2×6 cm) and placed onto the glass slide as shown in Figure 1. The average diameter of the nanopillar was approximately 100 nm.

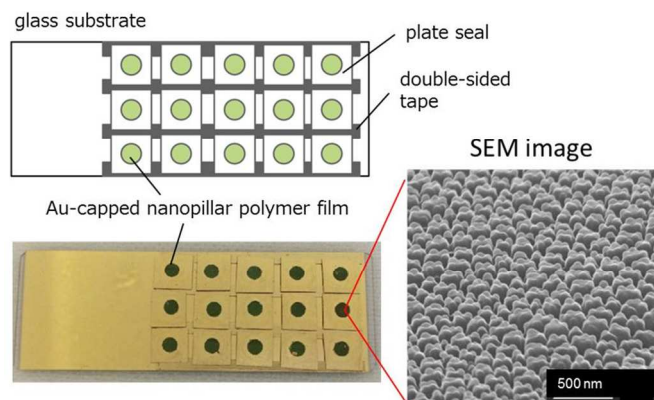


Fig. 1 Schematic illustration and images of a multi-array chip

Immobilization of the antibody onto the multi-array chip

For the immobilization of the antibody onto the multi-array chip, the self-assembly monolayer (SAM) was modified on the Au surface of the chip. An ethanol solution (1 mM) of 10-carboxy-1-decanethiol (Dojindo Molecular Technologies, Inc.) was dropped on the surface of the Au layer and kept for 1 h. Carboxyl groups of SAM were activated by casting 100 mM of N-hydroxysuccinimide (NHS, Wako Pure Chemical Industries, Ltd.) solution and 400 mM of water soluble carbodiimide (WSC, Dojindo Molecular Technologies, Inc.) solution on the multi-array chip surface for 10 min. In this study, a goat anti-human IgA, a mouse anti-human C-reactive protein (CRP), and a goat anti-human transferrin (Bethyl Laboratories, Inc.) were immobilised on the sensor surface. A solution of $10 \mu\text{g/mL}$ of each antibody in phosphate buffered saline (PBS, pH 7.4) was dropped onto the SAM-functionalised surface and incubated for 1 h. Finally, a solution of 0.1% (w/v) albumin bovine serum (BSA, Sigma-Aldrich Co. LLC.) in PBS was added for 1 h to suppress nonspecific adsorption. The multi-array chip was washed with PBS containing 0.05% Tween 20 (PBST, pH 7.4) and dried with pure nitrogen gas at every step as required. All procedures were performed at room temperature.

Hyper-spectral imaging system

A schematic representation and pictures of the hyper-spectral imaging system of a multi-array chip are shown in Figure 2. The measurement system is based on a hyper-spectral imaging instrument composed of a thin-film tunable band-pass filter (TF-TBPF) system and a cooled CCD camera (BU-50LN, BITRAN Corp.). All measurement procedures of the system are

controlled by an original program developed on LabVIEW (National Instruments Corp.). First, the TBPF system is controlled. The TBPF system can cover a spectral range of 540–700 nm and functions as a 2-dimensional spectrometer. The light wavelength through the filter depends on the incident angle. By synchronising the motion of the filter and one frame acquisition of CCD camera, optical images at different wavelengths are sequentially obtained as shown in Figure 3(a). The mechanical movement of the TBPF system becomes a trigger for intermittent image acquisition by the cooled CCD camera. This operation flow ensures repeatability of the measurement. All images are provisionally stored as an imaging memory based on real time imaging frame acquisition. Images of the imaging memory are drawn offline to a PC through a USB port. The specification of the hyper-spectral imaging instrument was previously described in more detail²⁶. Images of the multi-array chip are acquired by this system through reduction optics with a telecentric imaging lens (0.16 \times , Telecentric 56675, Edmund Optics Inc.), so that the spectral image in the whole sensing area (2.5×4 cm), including 12–15 sensing spots, can be measured in one time acquisition.

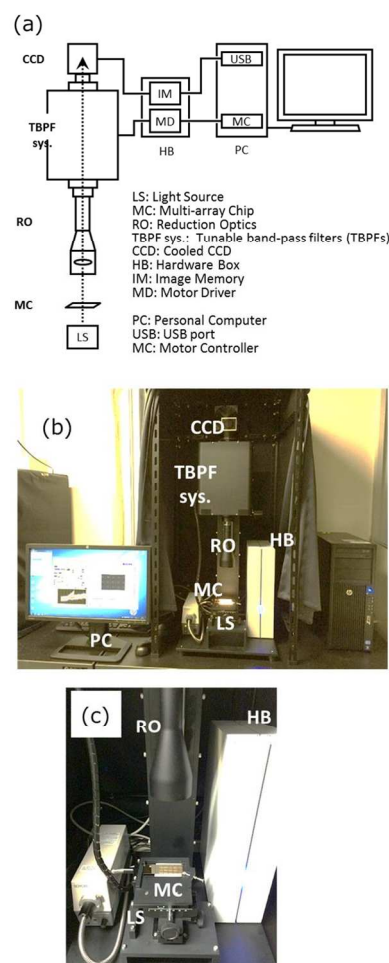


Fig. 2 Schematic (a) and overviews (b, c) of the hyper-spectral imaging system

Acquisition of spectral images

First, a dark spectral image was acquired by shuttering the incident light. The reference spectrum was acquired by a nanopillar film on a slide glass without Au deposition. This reference film was placed on the sample stage and a transmission spectral image was acquired by illuminating a white light from a halogen lamp (MI-150, Edmund Optics Inc.) from the backside. This spectral image was used as a reference for the calculation of the absorbance. Secondly, the reference film was replaced by a multi-array chip and the transmission spectrum image was acquired. Figure 3(a) shows images of the multi-array chip at wavelengths of 540, 620, and 700 nm. The absorption spectrum was obtained by converting a region of interest (ROI) spectrum with $50 \times 50 \mu\text{m}$ sized pixels to absorbance (Figure 3b). A LSPR band was clearly observed at around 565 nm in the absorption spectrum. ROI area could be optionally defined. In the case of the current multi-array, the analysed ROI area was 3.2 mm^2 (36×36 pixels). All spectra were measured in the spectral range of 540–700 nm with 0.5 nm of spectral interval.

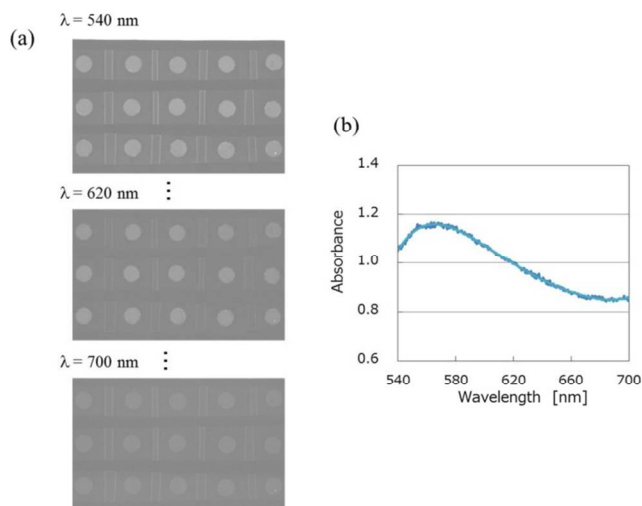


Fig. 3 Hyper-spectral images and an absorption spectrum at a sensing spot. (a) Representative images of a multi-array chip in a data set sequentially measured by the hyper-spectral imaging system. (b) An absorption spectrum of a sensing spot constructed from an image set (a).

Detection of the antigen-antibody reaction

We chose IgA and CRP as target molecules to test parallelized protein detections with our hyper-spectral imaging system, because their quantitative assays are clinically significant and they have been used in the study of a LSPR biosensing as we reported previously³. Figure 4(a) shows the schematic representation of the sensor chip in which anti-IgA and anti-CRP are immobilised on sensing spots. Human IgA and human CRP (Bethyl Laboratories, Inc.) were used as target antigen proteins. The antigen/PBS solution ($1 \mu\text{g}/\text{mL}$) was introduced onto each spot of the multi-array chip as shown in Figure 4a. After 1 h of incubation, the chip was washed with PBST and PBS and dried with pure nitrogen gas.

The absorption spectrum after exposure of the multi-array chip to the antigen was measured. The peak wavelength shift between before and after exposure to the antigens caused by antigen-antibody interaction was calculated. Figure 4(b) shows that the difference in the peak wavelength shift between the positive and negative control was clearly distinguished. The selectivity (specificity) and reproducibility are indicated in Figure 4(c). The error bars indicate standard deviations ($n = 3$). IgA and CRP sensing spots (anti-IgA and anti-CRP immobilized spots) show the large wavelength shift only for the application of respective antigens. This result demonstrates that multiple antigen-antibody interactions can be detected in a single measurement with high specificity by using the hyper-spectral imaging system and the Au-capped nanopillar chip.

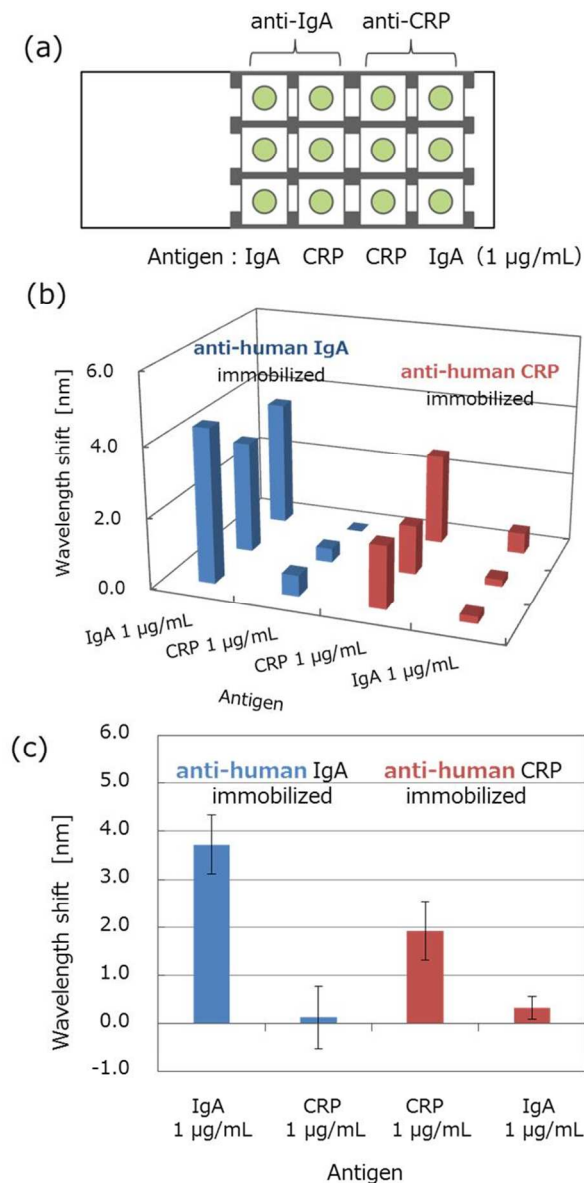


Fig. 4 Parallelized detection of IgA and CRP. (a) Representative images of a multi-array chip in a data set sequentially measured by the hyper-spectral imaging system. (b) An absorption spectrum of a sensing spot constructed from an image set (a).

Demonstration of a multiple quantitative assay

A multi-array chip was fabricated by using an anti-human IgA, anti-human CRP, and anti-human transferrin (TF) antibody as shown in Figure 5(a). After a blocking procedure, human IgA and human CRP solutions, 10 ng/mL to 10 μ g/mL in PBS, respectively, were introduced on the multi-array chip. The spectral image was measured after 1 h of incubation. The peak wavelength shift calculated at every spot is graphed in Figure 5(b) and (c). Specific binding of human IgA and human CRP to their respective antibody was detected and the values of the wavelength shift corresponded to the antigen concentrations.

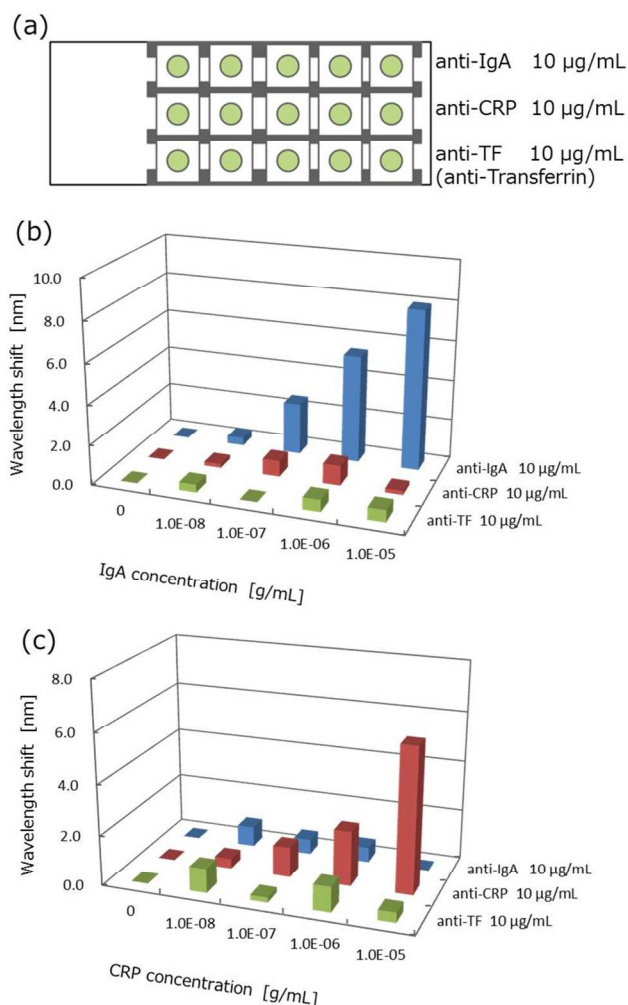


Fig. 5 Quantitative detection of IgA and CRP. (a) Schematic representation of the chip design. Peak wavelength shifts after application of IgA (b) and CRP (c) solutions at each respective spot.

Fig. 5(b) and 5(c) indicate that IgA and CRP whose concentrations are higher than ~ 100 ng/mL were selectively detected. Selectivity, throughput, sensitivity, and limit of detection (LOD) of parallelized label-free detection of protein interactions should be evaluated in comparison with some previous reports. E. Ozkumur et al. demonstrated that 19 ng/mL of anti-rabbit IgG was specifically detected by using microarray chips with an optical interference properties²⁴. Pilarik et al. succeeded in the parallelized detection of human chorionic

gonadotropin (hCG) and activated leukocyte cell adhesion molecule (ALCAM) by using surface-plasmon resonance (SPR) sensor chips and estimated limits of detection at 45 and 100 ng/mL, respectively⁶. The sensitivity of the present study is comparable or slightly lower than these previous reports. We think the sensitivity is limited by the non-specific binding of proteins and could be improved by the optimization of the chip fabrication. It should be noted that a simple comparison with a previous work is quite difficult, because the sensitivity depends on the affinity of antigen-antibody interactions of target molecules. The throughput becomes higher by increasing the number of sensing spots on a chip. In principle, the number of spots processed by the spectral imaging system in one time is limited by the number of pixels of a CCD camera. The present system employs a CCD camera with 772×580 pixels and is capable of using another camera with a higher number of pixels. Thus the present assay can afford to greatly increase the throughput. In general, hyper-spectral imaging is attained by using a diffraction grating or a liquid crystal tunable filter^{17, 19}, which take a high cost as compared to a thin-film bandpass filter used in our system. In the present study, we showed a proto-type system using multiarray chips with 12 -15 detection spots and commercial proteins as test targets. This is a preliminary work but an important step towards practical applications like high-throughput proteomics with real samples.

Conclusions

Multiple label-free detection of protein interaction was performed by using a hyper-spectral imaging system. Au-capped nanopillar polymer films fabricated by thermal nanoimprint lithography were used as platforms for multi-array LSPR sensor chips. IgA and CRP were specifically detected in a single measurement. Parallelized detection of multiple sensing spots saves time and labour and avoids the error due to the measurement time lag among sensing spots. The resolution of the hyper-spectral imaging system allows the process of a larger number of arrays. The increase in the number of proteins, which can be analysed at once, allows the enhancement of the throughput and performance of diagnostics based on biological assays.

Acknowledgements

This work was supported by the Nakatani Foundation of Electronic Measuring Technology Advancement and the Osaka University LLP (Lean LaunchPad Program) Gap Fund, which is conducted as part of the MEXT/JST EDGE program (Enhancing Development of Global Entrepreneur Program).

Notes and references

^aDepartment of Applied Physics, Graduate School of Engineering, Osaka University, 2-1 Yamadaoka, Suita, Osaka, Japan 565-0871.

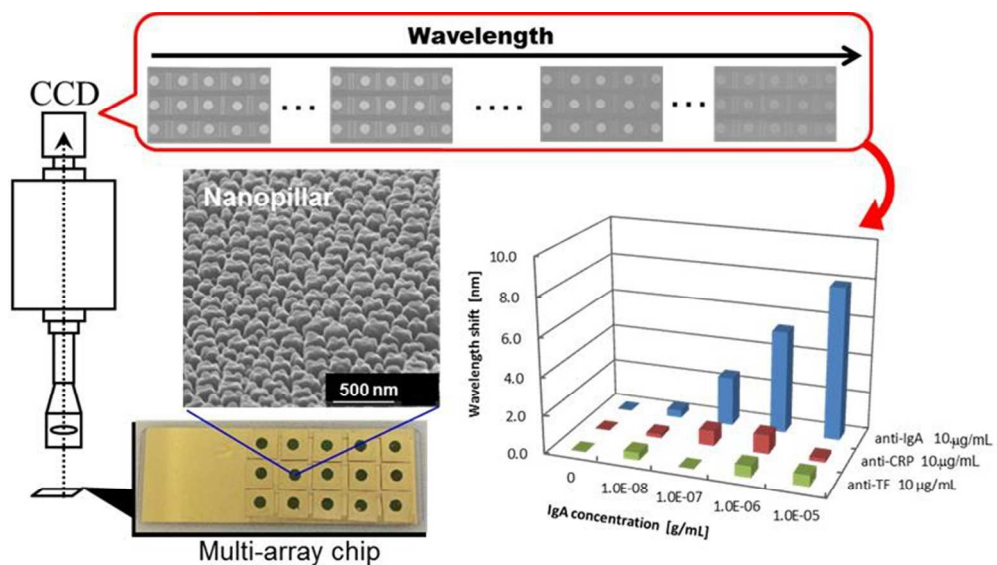
E-mail: yosikawa@ap.eng.osaka-u.ac.jp

^bInnovation Head Quarters, Yokogawa Electric Corporation, Musashino, Tokyo, Japan 180-8750.

1. A. Qureshi, J. H. Niazi, S. Kallempudi and Y. Gurbuz, *Biosens. Bioelectron.*, 2010, 25, 2318-2323.
2. M. S. Wilson and W. Y. Nie, *Anal. Chem.*, 2006, 78, 6476-6483.

Journal Name

3. T. Endo, K. Kerman, N. Nagatani, H. M. Hiepa, D. K. Kim, Y. Yonezawa, K. Nakano and E. Tamiya, *Anal. Chem.*, 2006, 78, 6465-6475.
4. J. Ji, J. G. O'Connell, D. J. D. Carter and D. N. Larson, *Anal. Chem.*, 2008, 80, 2491-2498.
5. G. Marusov, A. Sweatt, K. Pietrosimone, D. Benson, S. J. Geary, L. K. Silbart, S. Challa, J. Lagoy, D. A. Lawrence and M. A. Lynes, *Environ. Sci. Technol.*, 2012, 46, 348-359.
6. M. Piliarik, M. Bockova and J. Homola, *Biosens. Bioelectron.*, 2010, 26, 1656-1661.
7. S. Y. Chou, P. R. Krauss and P. J. Renstrom, *J. Vac. Sci. Technol. B*, 1996, 14, 4129-4133.
8. S. Y. Chou, P. R. Krauss and P. J. Renstrom, *Appl. Phys. Lett.*, 1995, 67, 3114-3116.
9. F. Buyukserin, M. Aryal, J. M. Gao and W. C. Hu, *Small*, 2009, 5, 1632-1636.
10. S. Y. Chou, P. R. Krauss, W. Zhang, L. J. Guo and L. Zhuang, *J. Vac. Sci. Technol. B*, 1997, 15, 2897-2904.
11. L. J. Guo, E. Leobandung, L. Zhuang and S. Y. Chou, *J. Vac. Sci. Technol. B*, 1997, 15, 2840-2843.
12. W. Wu, B. Cui, X. Y. Sun, W. Zhang, L. Zhuang, L. S. Kong and S. Y. Chou, *J. Vac. Sci. Technol. B*, 1998, 16, 3825-3829.
13. J. Wang, S. Schablitsky, Z. N. Yu, W. Wu and S. Y. Chou, *J. Vac. Sci. Technol. B*, 1999, 17, 2957-2960.
14. M. T. Li, J. A. Wang, L. Zhuang and S. Y. Chou, *Appl. Phys. Lett.*, 2000, 76, 673-675.
15. M. Saito, A. Kitamura, M. Murahashi, K. Yamanaka, L. Q. Hoa, Y. Yamaguchi and E. Tamiya, *Anal. Chem.*, 2012, 84, 5494-5500.
16. A. Yokoo, K. Wada and L. C. Kimerling, *Jpn. J. Appl. Phys. I*, 2007, 46, 6395-6397.
17. J. A. Ruemmele, W. P. Hall, L. K. Ruvuna and R. P. Van Duyne, *Anal. Chem.*, 2013, 85, 4560-4566.
18. O. Bleher, A. Schindler, M. X. Yin, A. B. Holmes, P. B. Lippa, G. Gauglitz and G. Proll, *Anal. Bioanal. Chem.*, 2014, 406, 3305-3314.
19. S. H. Lee, N. C. Lindquist, N. J. Wittenberg, L. R. Jordan and S. H. Oh, *Lab Chip*, 2012, 12, 3882-3890.
20. K. Tsuboi, S. Fukuba, R. Naraoka, K. Fujita and K. Kajikawa, *Appl. Optics*, 2007, 46, 4486-4490.
21. M. Piliarik, H. Vaisocherova and J. Homola, *Biosens. Bioelectron.*, 2005, 20, 2104-2110.
22. L. Liu, S. H. Ma, Y. H. Ji, X. Y. Chong, Z. Y. Liu, Y. H. He and J. H. Guo, *Rev. Sci. Instrum.*, 2011, 82.
23. E. Cho, R. Shin, J. Shim, H. I. Jung and S. Kang, *Appl. Phys. Lett.*, 2014, 105.
24. E. Ozkumur, J. W. Needham, D. A. Bergstein, R. Gonzalez, M. Cabodi, J. M. Gershoni, B. B. Goldberg and M. S. Unlu, *Proc. Natl. Acad. Sci. USA.*, 2008, 105, 7988-7992.
25. B. T. Cunningham, P. Li, S. Schulz, B. Lin, C. Baird, J. Gerstenmaier, C. Genick, F. Wang, E. Fine and L. Laing, *J. Biomol. Screen.*, 2004, 9, 481-490.
26. M. Iga, N. Kakuryu, T. Tanaami, J. Sajiki, K. Isozaki and T. Itoh, *Rev. Sci. Instrum.*, 2012, 83.



Parallelized detection of protein interactions using a multi-array chip and a hyper-spectral imaging system
70x40mm (300 x 300 DPI)